

FEATURE ARTICLE

Chemical Reactions in Clusters

Elliot R. Bernstein

Chemistry Department, Colorado State University, Fort Collins, Colorado 80523 (Received: June 30, 1992; In Final Form: September 10, 1992)

Four different classes of cluster chemical reactions are reviewed and specific examples from our laboratory are given for each class. Solvent-induced electron-transfer reactions are illustrated by our studies of 4-(dimethylamino)benzonitrile/acetonitrile clusters. The electron-transfer reaction depends on solvent polarity and on cluster structure. The reaction is induced by only one properly oriented CH_3CN solvent molecule. Proton-transfer reactions in neutral clusters are exemplified by the 1-naphthol/ammonia cluster system. Proton transfer occurs in the first excited singlet state of the 1-naphthol (NH_3)_n cluster of the proper geometry. Two time decays are measured for this event: one dealing with proton transfer and the other with "solvent reorganization or relaxation" following the transfer event. Isotope, energy, cluster size dependence, and model calculations demonstrate a proton tunneling mechanism is appropriate for this reaction. Cluster ion chemistry for toluene, toluene-*d*₃, benzyl alcohol, benzyl- α , α -*d*₂ alcohol, α , α -dimethylbenzyl alcohol/ammonia and water clusters is also discussed. These ionic reactions are characterized by benzyl-like radical formation, solvation of protons, and extensive cluster fragmentation following both ion formation and proton transfer. Finally, a preliminary study of radical reactions in clusters is presented for the benzyl radical clustered with ethylene, propylene, and acetylene.

Introduction

Elucidation of chemical reactions on a molecular level is a major focus of modern physical chemistry. In particular, a number of characteristics of the reactants and products are of interest: energy of the reacting species and its distribution between internal (rotation, vibration, electronic) and external degrees of freedom; geometry of the individual species; relative orientation of the reacting species; energy and its distribution within the identified product species; the reaction coordinate, transition state, barriers—the potential energy surface for the reaction; and changes in the above properties with solvation. Different subareas of physical chemistry are concerned with these aspects of chemical reactivity to varying degrees.

Clusters generated and isolated in a supersonic expansion can be employed to investigate many of these characteristics: clusters can be generated within a narrow range of temperatures; small clusters typically have resolvable energy levels and geometries; cluster size can be controlled and clusters of a particular size can be accessed and detected; clusters can be placed in particular electronic and vibrational energy levels and reactions can be initiated at a known time by photoexcitation; and nonreactive energy dynamics (intracuster vibrational redistribution, IVR; and vibrational predissociation, VP) can be predicted for clusters of different size (RRKM and phase space theories). Clusters can thus play a central role in the elucidation of solvation, solvation structure, transition states, reaction energy distribution, and potential energy surfaces for reactions.¹

Clusters of reacting or reactive molecules and intermediates can be generated in the now well-known manner by supersonic expansion into a vacuum system and their presence detected and properties elucidated by mass-resolved excitation, fluorescence, and dispersed emission spectroscopies.^{1c} Chemical reactions in clusters can be detected very much as chemical reactions in solutions can be detected, through comparison of the behavior of nonreactive "normal" systems with the behavior of reactive systems. For example, spectroscopic comparisons can be made between clusters of 4-(dimethylamino)benzonitrile (DMABN) with water (no electron transfer) and acetonitrile (electron transfer), naphthol with water (no proton transfer) and ammonia (proton transfer), benzyl radical with ethane (no reaction) and ethylene (possible reaction), etc. Specifically, for a cluster undergoing a

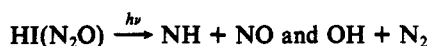
chemical transformation, one can characterize, as a function of cluster composition, size, or structure, a number of changes in the cluster spectroscopic properties. These include changes in emission, absorption, ionization cross sections, and relaxation dynamics as well as the appearance of new signals and species. Moreover, one can employ spectroscopy to analyze for the products of cluster chemical reactions. Examples of these changes are shown for the four systems discussed in the article. For the DMABN electron-transfer system, large spectroscopic changes occur for the clusters undergoing electron transfer: these include absorption and emission line width, large red shifts for both absorption and emission, and a change in lifetime of the emission. For proton transfer, both emission red shift and time dependence of the spectrum indicate the proton has indeed undergone a translocation. In the case of reactions in ionic clusters, the Franck-Condon factors for ionization and the enthalpy of reaction cause enough excess energy in the cluster such that fragmentation of the clusters occurs and actual product ions are directly observed.

Just what reaction has occurred in a cluster and what mechanism(s) might be appropriate to suggest for it can also be determined. One can employ product analysis, isotopic and chemical substitution effects on rates and mechanisms, and variation of reactant energy in the internal degrees of freedom to explore the nature and pathway of the observed reaction. For example, the best proof that proton transfer is occurring in a cluster can be found through H/D substitution: proton tunneling is dramatically influenced by changes in the mass of the tunneling particle. Additionally, H/D/ CH_3 isotopic and chemical substitution can be used to identify products and even reaction pathways for $\text{C}_6\text{H}_5\text{CR}^1\text{R}^2\text{R}^3(\text{H}_2\text{O})_n$ and $(\text{NH}_3)_n$ ionic cluster systems. These specifics will be presented in the discussion below.

Details of the study of chemical reactions in clusters depend heavily on the nature of the reaction that has taken place. The reactions that are of interest here are photoinduced reactions. Two different photoinduced reactions can be classified in general—adiabatic and diabatic. An adiabatic reaction, best exemplified by the excited-state electron-² and proton-transfer^{3,5} reactions discussed below, is one in which excited-state reactants generate excited-state products on "the same" potential energy surface. A diabatic reaction, best exemplified by [2 + 2] cycloaddition and hydrogen abstraction/diradical reactions,⁶ is one in which ex-

cited-state reactants generate ground-state products. To study an adiabatic photoinduced reaction, one photon is needed to excite the cluster following which the product can either emit or be further excited by a second photon to observe mass-detected spectra. To study a diabatic photoinduced reaction, two or three photons are required: one to initiate the reaction, one to reexcite the ground-state products following which the products can either emit or be further excited (ionized) by a third photon. If either of these reaction types involves a reactive intermediate (e.g., a radical, carbene, nitrene, etc.) that is photogenerated, an additional photon is required to generate the reactants for the cluster chemical reaction. Some cluster reactions occur in the cluster ion. These can be accessed by two photon excitation ($I \leftarrow S_1 \leftarrow S_0$) of the cluster and mass-resolved excitation spectroscopy. The products formed in these reactions depend on the cluster size, geometry and the amount of vibrational energy in the cluster ion ground electronic state.

Neutral cluster photoinduced chemistry (between a solute chromophore and a solvent molecule) has been previously reported. Wittig's group⁷ has studied the photoinduced reactions



The reaction is diabatic and the OH radical is probed through additional excitation and state-resolved fluorescence. Zewail's group⁸ has also studied such systems and has made time-resolved measurements of this and similar reactions. Proton-transfer reactions in the S_1 of clusters (e.g., phenol/ NH_3 and 1-naphthol/ NH_3) as well as electron-transfer reactions are additional examples of reactions in neutral clusters.^{2,3} The effect of clustering on the methyl iodide Rydberg state vibrational predissociation has also been investigated.^{4a,b} Other systems have also been reported.^{4c}

Chemical reactions in ionic solute/solvent clusters are more easily studied and have also been reported. Phenylacetylene/ammonia clusters⁹ and others^{9b,10} have been investigated for proton-transfer and substitution reactions have also been observed in ionic clusters.¹¹ More examples of solute/solvent cluster ion reactions will be discussed below. Single component cluster ion chemistry is also well studied.^{9b,10} Related studies on electron detachment for negative ion clusters, recombination reactions in negative ion clusters, and photoelectron studies of large negative ion cluster chemistry are also reported in the literature.^{10e-h} We mention these parallel studies in similar areas to apprise the interested reader of additional efforts in cluster chemical reactions and selection behavior.

In this paper, we present a review of a number of cluster chemical reactions studied in our laboratory and also present some preliminary investigations of new systems. The cluster reactions we will address include electron transfer (4-(dimethylamino)-benzonitrile with polar solvents), excited-state proton transfer (1-naphthol with ammonia), cluster ion proton transfer and radical chemistry (toluenes and benzyl alcohols with water and ammonia), and neutral cluster radical chemistry (benzyl radical with olefins). Qualitatively accurate model potential energy surfaces for both excited-state electron- and proton-transfer reactions are presented and discussed.

Experimental Procedures

In general, the experimental procedures for mass-resolved and fluorescence excitation spectroscopies (MRES and FE) of molecules and clusters are well described in the literature.¹² Two variations of these techniques should be mentioned here to highlight the study of chemical reactions in clusters.

As pointed out in the Introduction, the nature of the experimental apparatus used for the study of cluster chemistry depends on the nature of the photoinduced reaction (diabatic vs adiabatic) and the nature of the reacting species (stable molecule or reactive intermediate). Basically these conditions and constraints control the number of lasers needed to generate the experimental results. These various cases are illustrated in Figure 1. Figure 2 shows

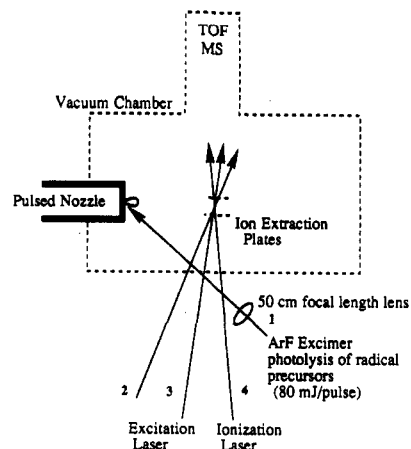


Figure 1. Arrangement of lasers for the investigation of photogenerated reactive intermediates in clusters. The excimer laser points to the expansion nozzle and photolyzes the volatile precursors during the initial stages of the expansion. The radicals, etc. cool and condense with solvent molecules in the expansion gas. Excitation lasers 2, 3, 4 are used to initiate reactions and detect products as required for different types of reactions. See text for more details.

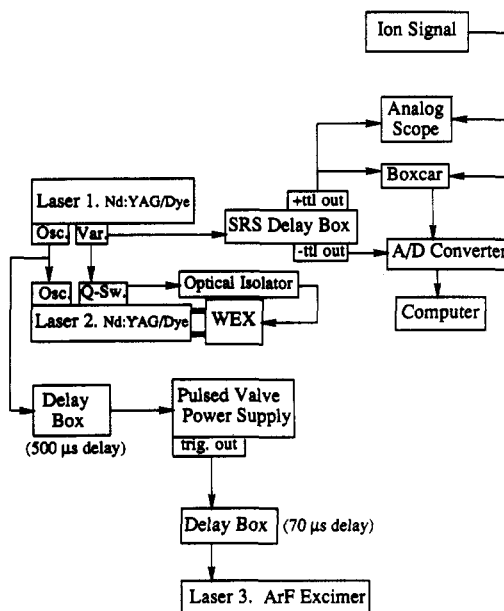


Figure 2. Electronic and timing arrangement for the experiments described in Figure 1.

the timing and detection sequence for the three-photon, adiabatic reaction MRES experiment or the diabatic reaction fluorescence excitation experiment involving a photogenerated reactive intermediate.

In our experiments, the tunable dye lasers are three separate Nd/YAG pumped dye lasers which can cover the wavelength range from 750 to 217 nm. The photolysis laser is an excimer laser which typically is used with an Ar/ F_2 active medium (193 nm). While the timing of the three- and four-laser experiment can be challenging, the other aspects of the procedure are straightforward and present little difficulty. The details of such experiments are presented in ref 13.

An important component of the study of chemical reactions in clusters is identification of individual cluster size. This is typically not a difficult task if mass-resolved spectroscopy is employed; however, in a reacting cluster both the transition Franck-Condon factors and the exothermicity of the reaction can give rise to cluster fragmentation and, thereby, loss of mass resolution for the cluster system.^{11,14} The experimental technique we have employed to circumvent this difficulty involves nozzle/laser timing delay measurements. The idea behind this experiment is that the larger a cluster is the longer it takes to form

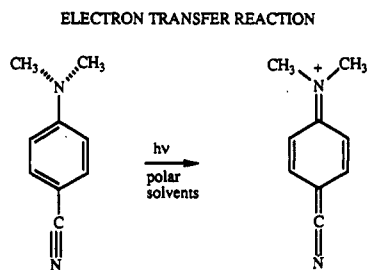


Figure 3. A schematic depiction of a (polar) solvent-assisted electron-transfer reaction for 4-DMABN.

in the expansion and the slower it must travel. Thus, the first species to reach the MRES detection region is the isolated solute, followed in time by solute/(solvent)_n clusters in order of increasing *n*. In our apparatus, the clusters (mass ca. 125 amu) are separated initially by ca. 5 μs. As clusters become larger this separation reduces: at about *n* = 5 this separation becomes 2–3 μs for NH₃ or H₂O solvents. The method is quite successful in identifying clusters up to about *n* = 6 or 7 for toluene and benzyl alcohol clustered with NH₃ and H₂O.¹⁴

This approach works in the following manner. The nozzle is opened at a given time, and the lasers are then triggered to intercept the gas pulse at the mass spectrometer ionization region. The gas pulse is roughly 100 μs or 20 cm long. The distribution of clusters with respect to cluster mass is not homogeneous within this pulse: small clusters arrive at the nozzle before large ones because large clusters travel more slowly and take longer to form. If the lasers are triggered to probe this inhomogeneous distribution and specific mass channels are monitored as the nozzle/laser firing time is varied, one finds that clusters of various masses have different delay times at which they begin to appear. These times occur at regular and reproducible intervals which are characteristic of the cluster mass. Thus, a signal that may appear in the bare chromophore molecule mass channel can have the arrival time of a solute (solvent)_n cluster: this would identify the signal as coming from the solute (solvent)_n parent cluster and fragmenting upon cluster ionization. More details can be found in the original publications of this technique.¹⁴

Results and Discussion

A. Excited-State Electron-Transfer Reaction of 4-DMABN Clustered with Polar Solvents.² An electron-transfer reaction involves movement of an electron(s) and nuclei in a molecule such that the properties (e.g., charge distribution, multipole moments, polarizability, geometry, etc.) of the molecule become significantly and detectably altered. 4-DMABN undergoes such a change upon photoexcitation in the presence of acetonitrile, acetone, dichloromethane, and other polar non-hydrogen-bonding solvents. The reaction is schematically pictured in Figure 3. The solvent must stabilize not only the charge separation but also the nuclear relaxation/geometry change which accompanies the electron transfer. A simple model for such behavior can be constructed as follows: in the bare molecule and a cluster with a nonpolar solvent, 4-DMABN has an S₁(ππ*) state which is the lowest excited single state and a charge transfer (CT) excited state at considerably higher energy. In the presence of a polar solvent the S₁(ππ*) state is not greatly shifted, but the CT state is lowered in energy enough to become the lowest lying singlet state. Such processes are known to be important for the initial steps in many chemically and biologically important reactions.¹⁵

The S₁ ← S₀ origin region MRES of 4-DMABN is sharp, well-resolved, and reveals changes in both the inversion about the dimethylamino group nitrogen atom and the rotation of the dimethylamino group itself (see Figure 4). These features are not only found for 4-DMABN but many other dimethylamino aromatic species. Since 4-DMABN is the only molecule of this set for which the charge-transfer state is lowered below the local S₁(ππ*) by a polar solvent, this dual displacement motion of the dimethylamino group upon S₁ ← S₀ excitation is most likely unrelated to the CT process.

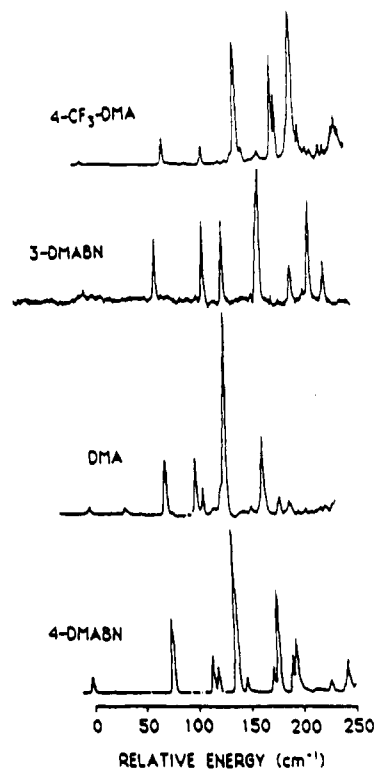


Figure 4. MRES of 4-DMABN and various similar molecules which show the S₁ ← S₀ origin region structure due to inversion and rotation of the dimethylamino group. DMA is *N,N*-dimethylaniline. The 4-DMABN origin (0) lies at 32 264 cm⁻¹.

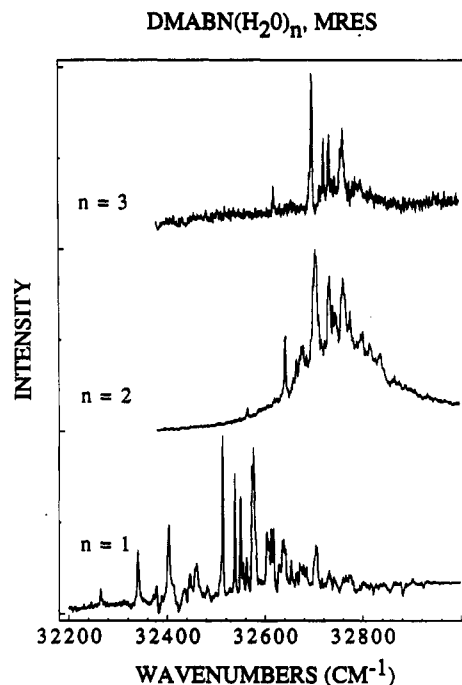


Figure 5. MRES of DMABN(H₂O)_{1,2,3}. The *n* = 1 spectrum is composed of transitions for clusters of two different geometries.

Clusters of 4-DMABN with methane and water show spectra similar to that of the bare molecule. In Figure 5, 4-DMABN-(H₂O)_{1,2,3} cluster spectra are presented which demonstrate this point. Saturation ion-dip experiments^{2c} clearly demonstrate that two 4-DMABN(H₂O)₁ clusters of different geometries are present in the beam. One can suggest that neither of these structures involves the water molecule bonded directly to the dimethylamino group because the bare molecule and cluster spectra, reflecting the compound motion of this group, are so similar.

The spectra of 4-DMABN clusters with non-hydrogen-bonding polar solvents, such as CH₃CN, (CH₃)₂CO, CH₂Cl₂, are com-

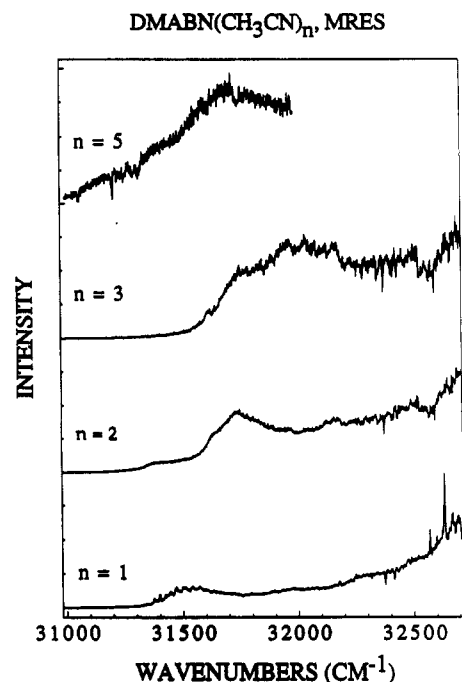


Figure 6. MRES of $\text{DMABN}(\text{CH}_3\text{CN})_n$, $n = 1, 2, 3, 5$. Note resolved features for $n = 1$ near $31\,500$ and $32\,600\text{ cm}^{-1}$. The latter set is due to a cluster of different geometry from the one generating the rest of the spectrum. The negative going features near $32\,300\text{ cm}^{-1}$ are due to monomer 4-DMABN.

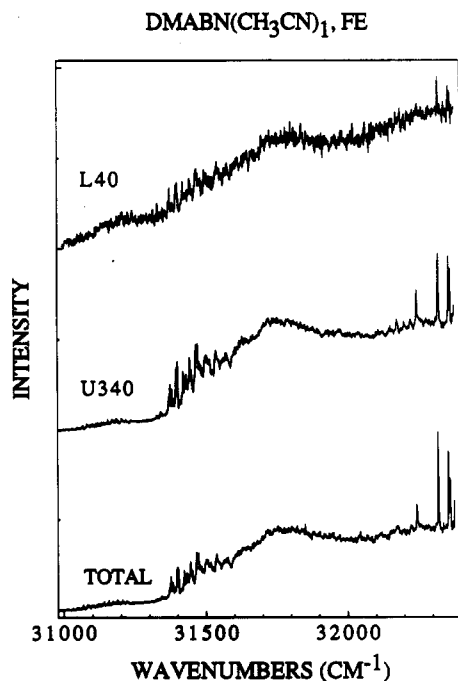


Figure 7. Fluorescence excitation spectra of $4\text{-DMABN}(\text{CH}_3\text{CN})_1$ obtained with different filters. The U340 filter essentially passes all the emitted light while the L40 filter passes only visible light. Note the broad excitation feature emits almost exclusively in the visible and the sharp excitation features emit almost exclusively in the ultraviolet. The U340 and "total emission" spectra are nearly identical as the higher energy states do not emit.

pletely different from those presented in Figures 4 and 5. An example of this behavior is shown for $4\text{-DMABN}(\text{CH}_3\text{CN})_n$ clusters in Figure 6 (MRES) and Figure 7 (fluorescence excitation). These spectra evidence of number of important features that yield information about the local $S_1(\pi\pi^*)$ electronic state and the charge (electron)-transfer electronic state and their relative positions in the various clusters. First, for $\text{DMABN}(\text{CH}_3\text{CN})_1$, two clusters of different geometry are observed. One cluster has a sharp isolated molecule-like spectrum near $32\,600\text{ cm}^{-1}$ and the

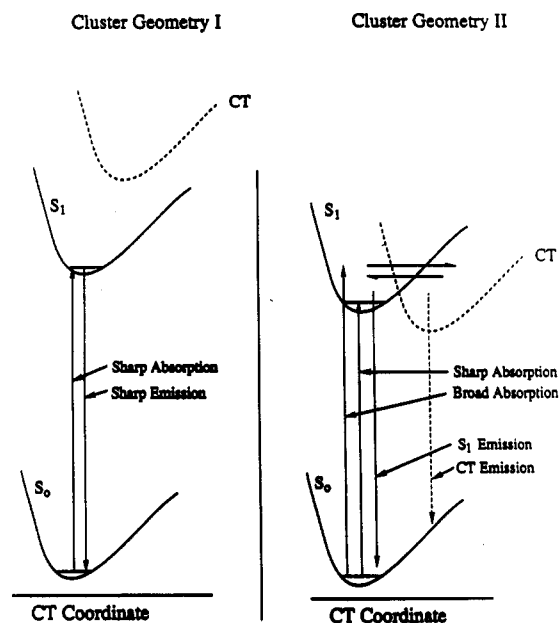


Figure 8. A schematic diagram of the potential energy surface of DMABN polar solvent cluster along the charge transfer coordinate. Cluster geometry I yields sharp blue shifted absorption with respect to the bare molecule. In this case, both excitation and emission spectra are well resolved, indicating little mixing of the CT state with the S_1 state: the CT state is not significantly stabilized with respect to the S_1 state. Cluster geometry II yields broad red-shifted absorption with respect to the bare molecule. In this geometry the S_1 and CT cluster states are both stabilized (lowered in energy) with respect to cluster S_0 state and are strongly mixed. Resolved features at the low-energy side of this red-shifted absorption are observed due to the small barrier in the CT coordinate between the S_1 and CT states. When the excitation energy is above the barrier, rapid evolution to the charge-transfer state occurs leading to a broad absorption spectrum. As intracenter vibrational redistribution from the DMABN modes to the van der Waals modes occurs the cluster will be trapped in either an S_1 -like or a CT-like excited state. Two emission lifetimes are thus expected for the cluster.

other has a very broad spectrum commencing at $31\,400\text{ cm}^{-1}$ and extending to higher energy. This latter spectrum shows some resolvable features between $31\,400$ and $31\,600\text{ cm}^{-1}$. These assignments follow from saturation ("hole-burning") ion-dip experiments described previously. Second, fluorescence excitation spectra detected at different wavelengths show different structures implying that the two clusters of $\text{DMABN}(\text{CH}_3\text{CN})_1$ have different electronic properties. The emission coming from the broad absorption is significantly red-shifted compared to that of the bare molecule and the acetonitrile cluster with sharp spectra.

Empirical atom-atom potential calculations of the possible geometries for these water and acetonitrile clusters² have been carried out. The results of such calculations suggest that water coordinates to the CN moiety of DMABN (with a number of different geometries) and that CH_3CN coordinates both to the ring and the CN moieties. These calculations are not as helpful as they might be because multiple geometries with similar binding energies are obtained and the detailed structures are dependent on the atomic partial charges and the other parameters of the Lennard-Jones-Coulomb or exponential-six-Coulomb potentials chosen.

These results, along with lifetime measurements,^{2c} suggest that the overall photophysics and photochemistry of 4-DMABN clusters with polar and nonpolar solvents can be rationalized by ground (S_0) and excited ($S_1(\pi\pi^*)$ and CT) state potential surfaces as depicted in Figure 8. The figure specifically applies to the two $4\text{-DMABN}(\text{CH}_3\text{CN})_1$ cluster structures but the cluster geometry I surfaces are applicable to both the bare molecule and other clusters with sharp, isolated molecule-like spectra. The surfaces for cluster geometry II explain the initial resolved features in the broad excitation spectrum, the overall width of this spectrum, and the red-shifted emission. The lowest singlet excited-state surface for the 4-DMABN/polar non-hydrogen-bonding solvent

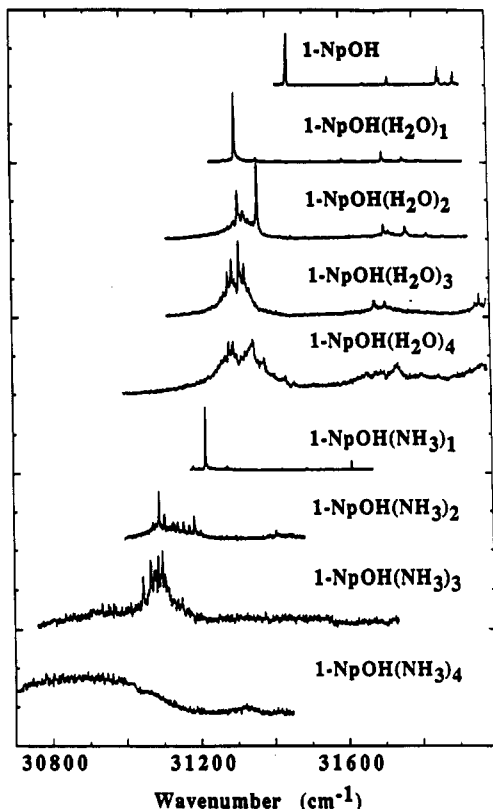


Figure 9. MRES of 1-naphthol, 1-naphthol(H_2O)_{1,2,3,4}, and 1-naphthol(NH_3)_{1,2,3,4} as indicated. The spectra presented do not lead to an obvious conclusion concerning proton transfer.

cluster system is a mixture of the $\pi\pi^*$ local and electron-transfer excited-state bare molecule surfaces.

Summarizing these results, two geometries are observed for the 4-DMABN(CH_3CN)₁ cluster and only one of them evidences the electron-transfer process at the lowest excited singlet state energy. Geometry is very important for generating elementary cluster chemical reactions. This particular geometry, based on cluster calculations,² is probably one with the two molecular dipoles aligned antiparallel, with the solvent "on top of" the aromatic ring.

Clearly, short-range dipolar interactions stabilize the electron-transfer process and only one solvent molecule properly placed is sufficient to induce the low-energy electron-transfer excited state.

B. Excited-State Proton Transfer in 1-Naphthol/Ammonia Clusters.⁵ The 1-naphthol/ammonia cluster system is a well-established excited-state proton-transfer system. Red-shifted emission from 1-naphthol(NH_3)_{*n*}, $n \geq 4$, clusters has been attributed to the (solvated) naphtholate anion.^{3a} A single picosecond decay measurement has been reported which suggests that excited-state proton transfer occurs for the $n = 3$ cluster.^{3c} Ionization threshold measurements show that two $n = 3$ clusters can be identified: one which has a high ionization energy as do the $n = 1, 2$ (and all water) clusters, and one which has a low ionization energy like the $n \geq 4$ ammonia clusters.^{5b} In addition to the above ionization energy study, we have performed a number of picosecond time-, wavelength-, and mass-resolved excitation experiments as a function of isotopic substitution, energy in the S_1 state of the cluster and ionization energy which are discussed below.^{5c}

The occurrence of proton transfer for one geometry of the 1-naphthol(NH_3)₃ cluster is not obvious from a comparison of its $S_1 \leftarrow S_0$ MRES with those of other 1-naphthol/ammonia and 1-naphthol/water spectra (see Figure 9), even though ionization threshold ($n \geq 3$) and emission energy ($n \geq 4$) suggest proton transfer can occur for this system. The proof of this conjecture comes from time- and mass-resolved cluster studies coupled with a theoretical model predicting the dependence of time-resolved results upon isotopic substitution (1-naphthol- $d(\text{ND}_3)_n$), increased vibrational energy in the S_1 state, and their dependence upon cluster size.

Using picosecond time- and wavelength-resolved two-color MRES, two relaxation times can be identified for the S_1 excited state of 1-naphthol(NH_3)_{3,4} clusters (see Figure 10). These times depend on cluster size, hydrogen isotope composition, and the vibrational energy in the cluster S_1 state. The data are summarized in Table I.

A model to explain these decay results can be constructed based on a proton-transfer event (τ_1) followed by solvent reorganization (τ_2). Both motions must change the cluster ionization cross section as the reaction coordinate evolves or no signal decay would be observed. The biexponential decay reflects the two-step nature of the evolution of the reactants (1-naphthol(NH_3)_{3,4} in the S_1 state) to the products (solvated 1-naphtholate anion and proton in the S_1 state). The proton must be transferred at the reactant-like

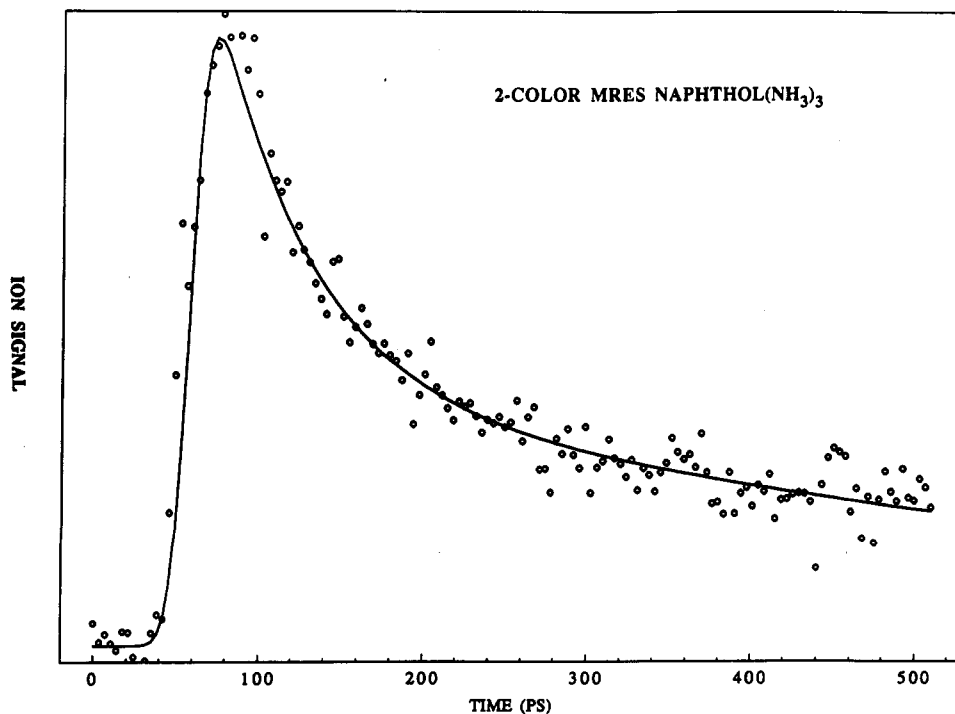


Figure 10. Decay curve for 2-color MRES of 1-naphthol(NH_3)₃ excited at 31 100 cm^{-1} and ionized at 29 000 cm^{-1} . The data points are the zeros, and the line is a biexponential fit to the data with $\tau_1 = 60$ ps and $\tau_2 = 500$ ps.

TABLE I: Experimental and Theoretical Decay Times for the Proton-Transfer Event (τ_1) and Subsequent Solvent Reorganization (τ_2) for 1-Naphthol(NH_3) $_n$ ($n = 3, 4$)

cluster	excitation energy (cm^{-1})	expt (ps)		calc ^a (ps)
		τ_1	τ_2	τ_1
$n = 3$; H	0_0^0	57	440	57
	+900	43	500	28
	+1400	12	120	13
D	0_0^0	>1000		2600
	+1400	75	>1000	200
$n = 4$; H	0_0^0	70	800	
	+1200	70	600	
	+1700	33	1000	

^a $E_0 = 6500 \text{ cm}^{-1}$, $a_0 = 0.2 \text{ \AA}$, $E(\text{OH}) = 3000 \text{ cm}^{-1}$, $E(\text{vdW}) = 110 \text{ cm}^{-1}$. The potential parameters are generated by fitting the proton-transfer time τ_1 to the 0_0^0 , $n = 3$, H data. $E(\text{OH})$ is estimated and $E(\text{vdW})$ is calculated for the cluster as given in ref 5d.

solvation and the cluster must then relax to a product-like solvation. Figure 11 presents a potential curve to model the proton-transfer event (τ_1) for this overall reaction. This function can account for the large isotope effect on the transfer rate, the cluster size effects observed, and the cluster vibrational energy dependence of the transfer rate.

The model proposed includes a harmonic well for the O-H stretch, a barrier of a given height and width (E_h , $2a$) between the O-H and H-N equilibrium positions for the reaction coordinate, proton transfer via a barrier penetration/tunneling mechanism, and use of the WKB approximation for the proton tunneling through the barrier along the reaction coordinate. Specifically, the rate constant for proton transfer can be written as

$$k = \nu \exp\left[-\frac{a\pi}{\hbar}(2mE_h)^{1/2}\right] \quad (1)$$

in which ν is the zero-point frequency for the proton in the potential well and m is the mass of the tunneling particle. The instantaneous barrier height and half-width are approximately related to their respective equilibrium values by^{5d}

$$E_h = E_0 \left(1 + \frac{x}{2a_0}\right)^2$$

and

$$a = a_0 \left(1 + \frac{x}{2a_0}\right)$$

For vibrational energy in the cluster this rate constant for proton transfer must be averaged over the O...N stretch van der Waals mode

$$k(v) = \langle \varphi_v | k(a) | \varphi_v \rangle \quad (2)$$

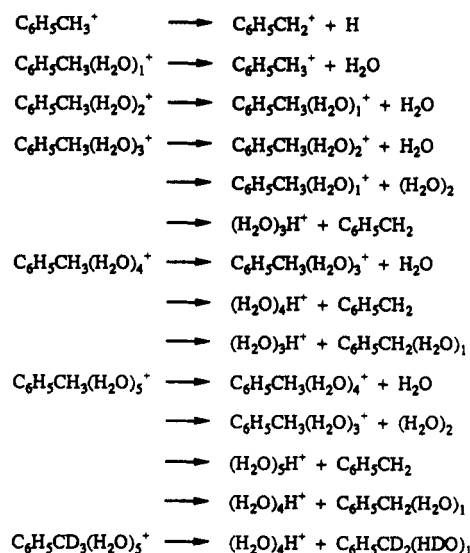
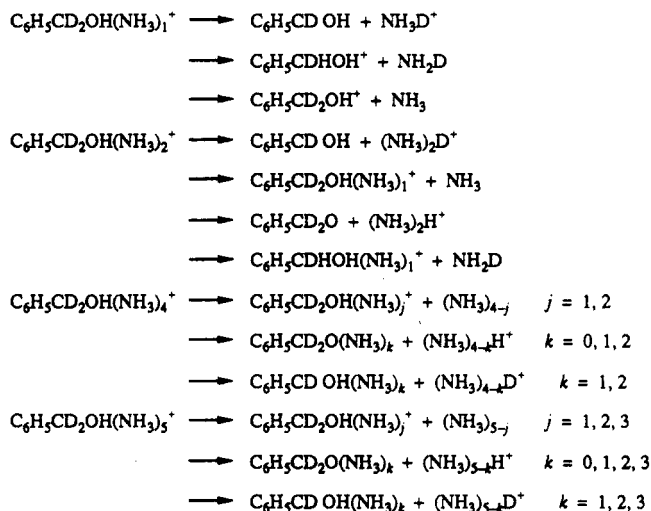
in which v is the number of quanta in the O...N stretch van der Waals mode. The probability that a specific van der Waals mode will be populated as a function of vibrational energy in the cluster is

$$P_v = \left[\frac{E - E_v}{E}\right]^{S-2} / \sum_v \left[\frac{E - E_v}{E}\right]^{S-2} \quad (3)$$

in which E is the vibrational energy in the cluster, E_v is the energy of the mode of interest, and S is the number of van der Waals modes in the cluster. Finally, the rate constant for proton transfer as a function of cluster vibrational energy is given by

$$k(E) = \sum_v P_v k(v) \quad (4)$$

The τ_1 value for the 1-naphthol(NH_3) $_3$ 0_0^0 excitation proton-transfer rate can be employed to calibrate this calculation and all other rates can be based on this one. The agreement between calculated and observed proton-transfer times (k^{-1}) is qualitatively

SCHEME I: Observed Fragmentation for Toluene/Water Clusters**SCHEME II: Observed Fragmentations for Benzyl Alcohol/Ammonia Clusters^a**

^aThe unobserved neutral fragment species, though written as an aggregate, may be individual molecules.

excellent as can be seen in Table I.

We are presently refining this model with further experimental studies on substituted naphthols and phenols and by better descriptions of the cluster vibrational space and geometry.

C. Cluster Ion Chemistry: Toluene and Benzyl Alcohols with Ammonia and Water.¹⁴ The chemistry of ions is, of course, very different from the chemistry of neutrals.^{10,11} The chemistry of ions is strongly influenced by solvation. Both these points are well illustrated by the series of reactions documented by the study of the cluster ion chemistry of toluene, benzyl alcohol, and α,α -dimethylbenzyl alcohol solvated by ammonia and water ($n = 1, \dots, 7$). The first realization of the extensive ion chemistry for these systems comes from the one- and two-color MRES presented in Figures 12-18. These data represent a spectacularly complex and initially confusing set of spectra for the various clusters. Only a small but representative portion of the total data for these clusters is presented here. A more complete data set can be found in the original publications. Employing different ionization energies, nozzle/laser timing delay experiments, isotopic substitution, and nanosecond time resolved measurements, parent clusters and various reaction paths can be identified. All the observed features have lifetimes that are commensurate with the S_1 lifetime of the isolated molecule species, and therefore all chemistry is initiated through $\text{I} \leftarrow S_1(0_0^0) \leftarrow S_0(0_0^0)$. Schemes I-IV show the cluster ion reactions that can be identified.

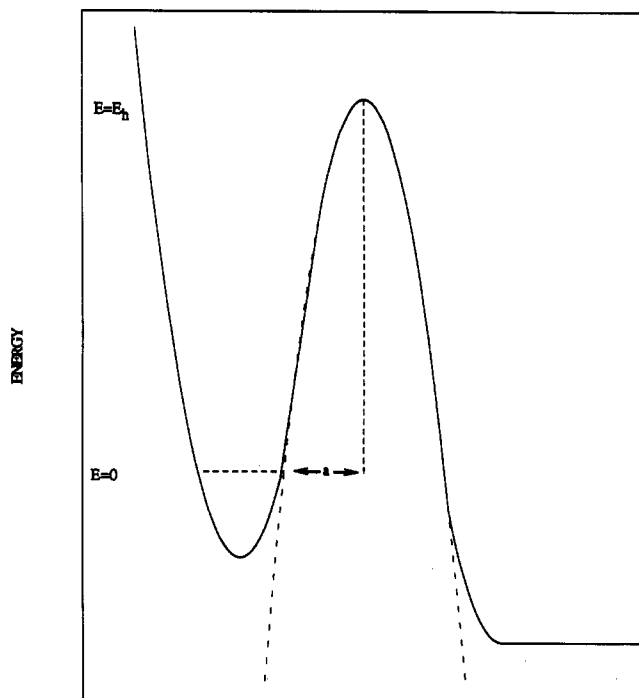


Figure 11. Schematic diagram of the potential model used for proton-transfer rate calculations. The dashed curve is the parabolic barrier using parameters fit to origin $n = 3$ data. The solid curve is the barrier model including a harmonic potential well with an OH vibrational energy of 3000 cm^{-1} . The well is centered at 1.0 \AA . The other parameters for this model are $E_0 = 6500 \text{ cm}^{-1}$, $a_0 = 0.2 \text{ \AA}$, and the van der Waals stretch energy is 110 cm^{-1} for 1-naphthol(NH_3)₃.

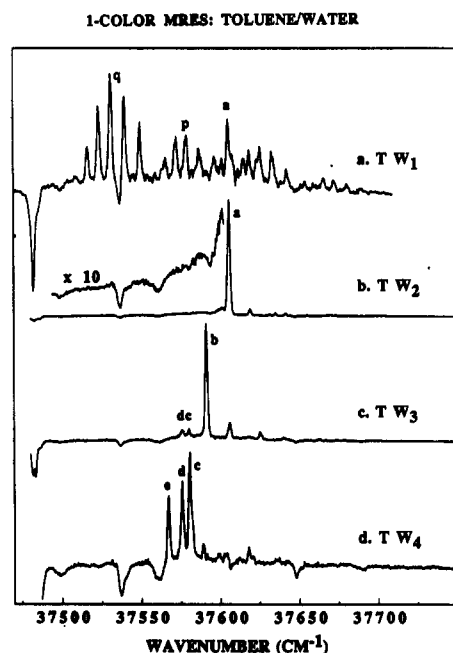


Figure 12. One-color mass-resolved excitation spectra of toluene/water clusters observed in the toluene(H_2O) _{n} -1 mass channels: (a) toluene(H_2O)₁, (b) toluene(H_2O)₂, (c) toluene(H_2O)₃, and (d) toluene(H_2O)₄. The mass channel designations in the figure (TW_m) refer to the detection channels not the true parent cluster masses. The parent clusters fragment following ionization as discussed in the text. In each spectrum TW_m^+ is detected. The negative peaks in the spectra are due to detector overload caused by very intense features associated with the bare molecule mass channel at the particular laser energy indicated by the wavenumber axis.

Consider first the spectra presented in Figures 12, 13, and 14 for the toluene/water cluster ion system. The spectra displayed arise from the $0_0^0 S_1 \leftarrow S_0$ transition of the toluene/water clusters

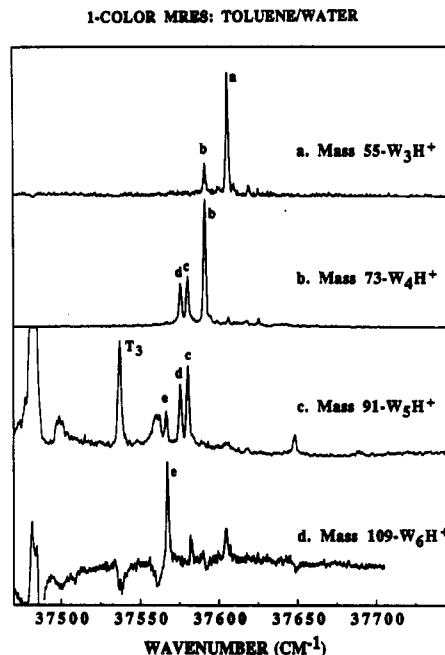
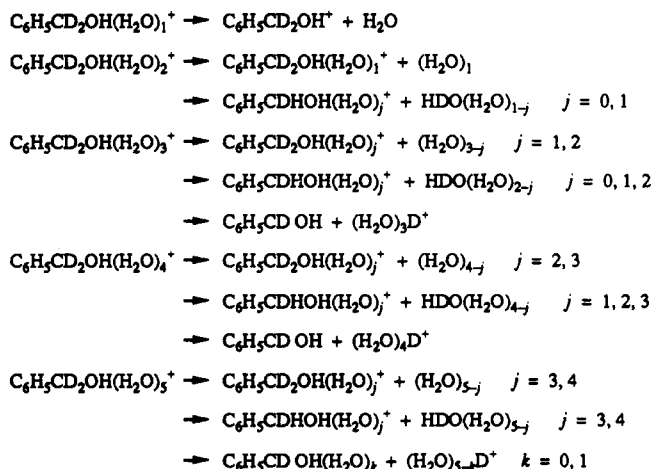


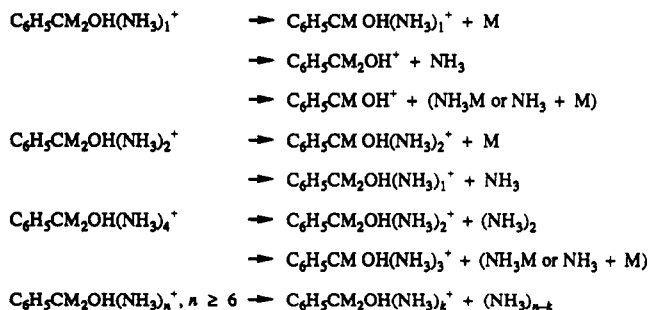
Figure 13. One-color mass-resolved excitation spectra of toluene/water clusters observed in (H_2O) _{x} H^+ mass channels: (a) (H_2O)₃ H^+ , (b) (H_2O)₄ H^+ , (c) (H_2O)₅ H^+ , and (d) (H_2O)₆ H^+ .

SCHEME III: Observed Fragmentations for Benzyl Alcohol/Water Clusters^a



^aThe unobserved neutral fragment species, though written as an aggregate, may be individual molecules.

SCHEME IV: Observed Fragmentations for α,α -Dimethylbenzyl Alcohol/Ammonia Clusters^a



^aThe unobserved neutral fragment species, though written as an aggregate, may be individual molecules.

for toluene(H_2O) _{n} , $n = 1, \dots, 6$. Even at the lowest possible ionization energy, extensive cluster fragmentation is observed. The major qualitative conclusions to be reached from these three sets of mass-resolved spectra are that specific $S_1 \leftarrow S_0$ cluster transitions (e.g., a, b, c, d, e, ...) occur in many different mass channels

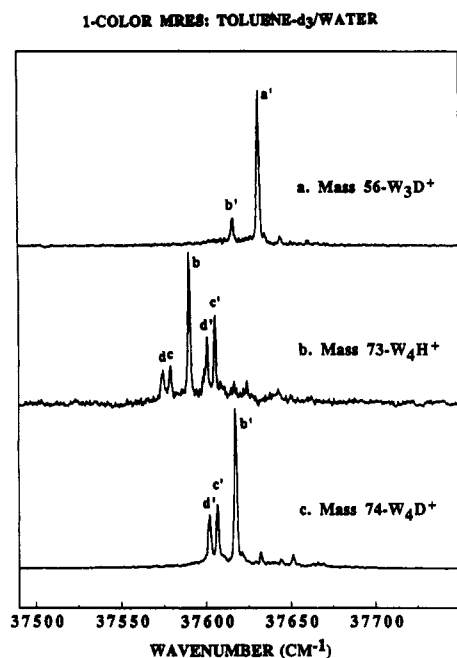


Figure 14. One-color mass-resolved excitation spectra of toluene- d_3 /water clusters observed in $(\text{H}_2\text{O})_x\text{H}$ (or D) $^+$ mass channels: (a) $(\text{H}_2\text{O})_3\text{D}^+$, (b) $(\text{H}_2\text{O})_4\text{H}^+$, and (c) $(\text{H}_2\text{O})_4\text{D}^+$. Features are labeled with primed letters to correspond to features found for toluene $(\text{H}_2\text{O})_x$ clusters.

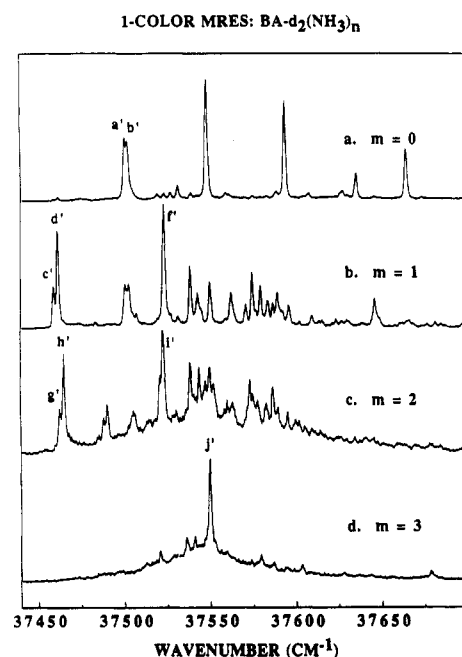


Figure 15. One-color mass-resolved excitation spectra of benzyl alcohol/ammonia clusters observed in the benzyl alcohol $(\text{NH}_3)_m$ mass channels: (a) benzyl alcohol, (b) benzyl alcohol $(\text{NH}_3)_1$, (c) benzyl alcohol $(\text{NH}_3)_2$, (d) benzyl alcohol $(\text{NH}_3)_3$, and (e) benzyl alcohol $(\text{NH}_3)_4$. The mass channel designations in the figure $\text{BA}(\text{NH}_3)_m$ refer to the detection channels and not the parent cluster channels. In each spectrum the $\text{BA}(\text{NH}_3)^+$ ion is detected.

and that the proton in the $(\text{H}_2\text{O})_m\text{H}^+$ cluster ion derives from the toluene molecule. The latter point is made by Figure 14 as the a' , b' , ... features are observed in the $(\text{H}_2\text{O})_m\text{D}^+$ mass channel. Moreover, since features d and c can be associated with the toluene $(\text{H}_2\text{O})_3$ cluster (Figure 13c), H/D exchange takes place in the clusters (Figure 14b). Thus, toluene- d_3 $(\text{H}_2\text{O})_3$ fragments upon ionization into the benzyl radical- d_2 $(\text{HDO})_1$ and $(\text{H}_2\text{O})_4\text{H}^+$, as well as the benzyl radical- d_2 $(\text{H}_2\text{O})_1$ and $(\text{H}_2\text{O})_4\text{D}^+$.

The mass-resolved spectra of Figure 15 and 16 show comparable behavior for a substituted toluene molecule (and benzyl radical), benzyl alcohol. Again, the clusters fragment at low ionization energy and the same O_0^0 spectral features are observed in a number

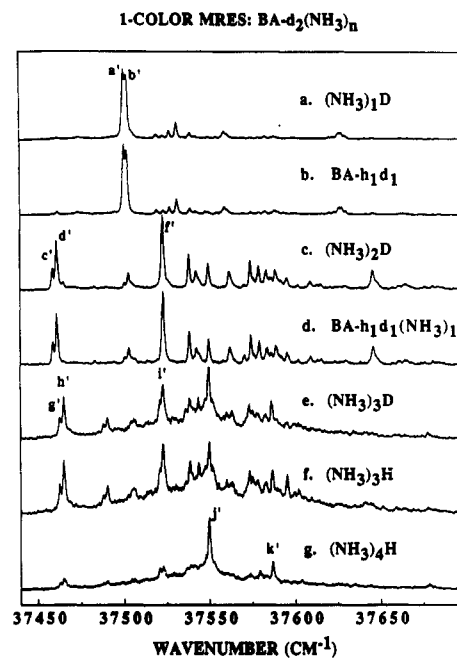


Figure 16. One-color mass-resolved excitation spectra of benzyl alcohol- d_2 /ammonia clusters observed in the following mass channels: (a) $(\text{NH}_3)_1\text{D}$, (b) benzyl alcohol- h_1d_1 , (c) $(\text{NH}_3)_2\text{D}$, (d) benzyl alcohol- $h_1d_1(\text{NH}_3)_1$, (e) $(\text{NH}_3)_3\text{D}$, (f) $(\text{NH}_3)_3\text{H}$, and (g) $(\text{NH}_3)_4\text{H}$. Features are labeled with primed letters corresponding to the undeuterated system. In each spectrum the positive ion is detected for the identified mass channel.

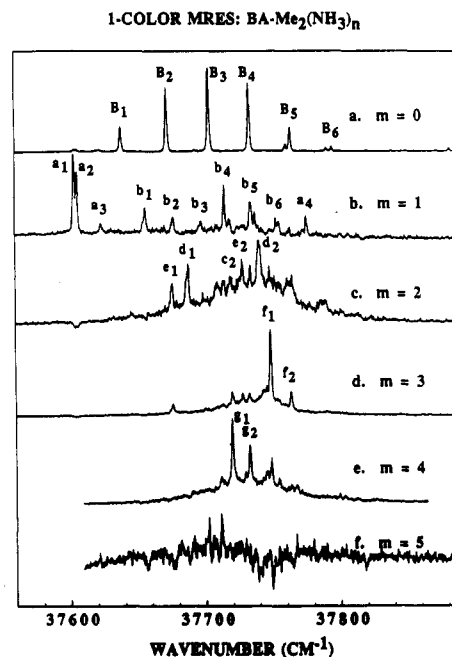


Figure 17. One-color mass-resolved excitation spectra of benzyl alcohol- Me_2 /ammonia clusters observed in the benzyl alcohol- $\text{Me}_2(\text{NH}_3)_m$ mass channels: (a) benzyl alcohol- Me_2 , (b) benzyl alcohol- $\text{Me}_2(\text{NH}_3)_1$, (c) benzyl alcohol- $\text{Me}_2(\text{NH}_3)_2$, (d) benzyl alcohol- $\text{Me}_2(\text{NH}_3)_3$, (e) benzyl alcohol- $\text{Me}_2(\text{NH}_3)_4$, and (f) benzyl alcohol- $\text{Me}_2(\text{NH}_3)_5$. The positive ion associated with the identified mass channel is detected.

of different mass channels. Compare, for example, Figures 15a and 16a,b, 15b and 16c,d, etc., to see that the a and b features for the benzyl alcohol/ammonia clusters are associated with clusters at least as large as benzyl alcohol $(\text{NH}_3)_1$.

Figure 16 demonstrates another interesting aspect of this cluster ion chemistry for benzyl alcohol/ammonia clusters. As the cluster becomes larger alcohol-proton transfer chemistry begins to occur rather than benzyl radical formation. Finally, for the higher mass channels only the alcohol-proton transfer reaction is observed: cluster ion chemistry is thus dependent on cluster size or the nature of the ion solvation.

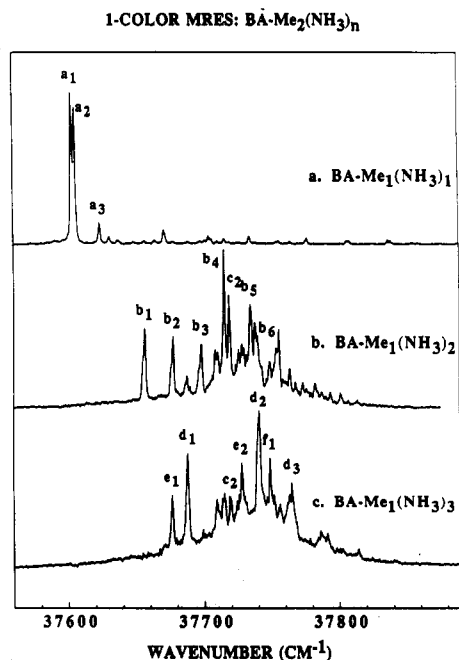


Figure 18. One-color mass-resolved excitation spectra of benzyl alcohol-Me₂/ammonia clusters observed in the benzyl alcohol-Me₁(NH₃)_n mass channels: (a) benzyl alcohol-Me₁(NH₃)₁, (b) benzyl alcohol-Me₁(NH₃)₂, and (c) benzyl alcohol-Me₁(NH₃)₃. The positive ion associated with the identified mass channel is detected.

The mass-resolved spectra of Figures 17 and 18 show a particularly surprising result: the benzyl alcohol-Me₂(NH₃)_n clusters generate upon ionization a substituted benzyl radical and a methyl radical. This system is never observed to transfer a proton from the alcohol moiety to the ammonia cluster.

A number of particularly interesting processes can be identified for these clusters and they are highlighted and summarized below.

1. toluene/water
 - a. cluster ion fragmentation for clusters of all sizes
 - b. cluster ion dissociative proton transfer to generate (H₂O)_mH⁺ ($m \geq 3$) and a benzyl radical
 - c. cluster ion dissociative proton transfer with H/D exchange among the water molecules
2. toluene/ammonia
 - a. cluster ion fragmentation
 - b. cluster ion dissociative proton transfer to form (NH₃)_kH⁺ ($k \geq 1$) and a benzyl radical
 - c. cluster ion dissociative proton transfer with H/D exchange among the ammonia molecules
3. benzyl alcohol (BA and BA- α , α -d₂)/water
 - a. cluster ion fragmentation for clusters of all sizes
 - b. cluster ion hydrogen transfer from the C α -position
 - c. cluster ion proton transfer from the C α -position to generate a substituted benzyl radical and (H₂O)_mH⁺ ($m \geq 3$)
 - d. cluster ion hydrogen exchange at the C α -position
4. benzyl alcohol (BA and BA- α , α -d₂)/ammonia
 - a. cluster ion fragmentation for clusters of all sizes
 - b. cluster ion hydrogen atom and proton transfer from the C α -position
 - c. cluster ion proton transfer from the OH moiety
 - d. cluster ion hydrogen exchange at the C α -position
5. benzyl alcohol- α , α -Me₂ (BA- α , α -Me₂)/ammonia
 - a. cluster ion fragmentation
 - b. cluster ion generation of methyl and substituted benzyl radicals

These reactions are all a function of cluster size, and indeed their relative significance changes as the clusters grow and the solvents become more basic. In particular, for small BA⁺(NH₃)_n clusters only the C α -proton transfers, but for larger clusters both the C α and OH protons transfer, with the acid-base (not the radical) chemistry becoming dominant for the larger clusters. Also, hydrogen exchange is more prevalent for small clusters. Note

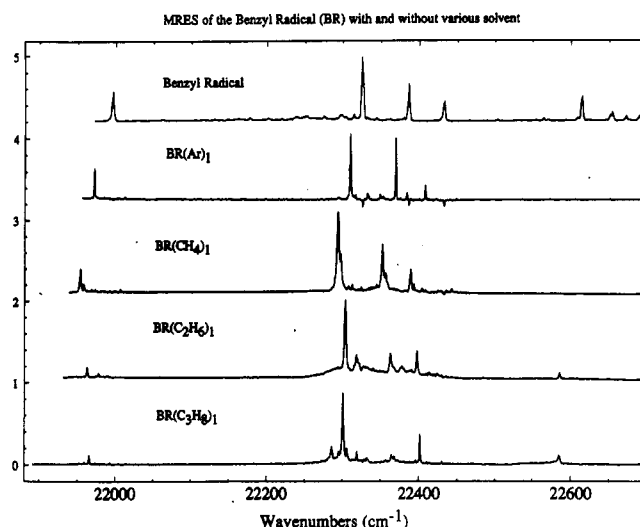


Figure 19. Two-color MRES of benzyl radical, benzyl radical (Ar)₁, benzyl radical (CH₄)₁, benzyl radical (C₂H₆)₁, and benzyl radical (C₃H₈)₁. The spectra show the D₁ ← D₀ (¹A₂ ← ¹B₂) transition at ca. 22 000 cm⁻¹ and the D₂ ← D₀ (²B₂ ← ¹B₂) at ca. 22 300 cm⁻¹. Clusters undergo dissociation at 500–700 cm⁻¹ above the cluster D₁ electronic origin.

too that at least three water molecules are required to solvate a proton whereas only one ammonia molecule will solvate a proton. Apparently, for water clusters up to $n = 6$ or 7 , water is not basic enough or a good enough solvent to generate C₆H₅CH₂O.

This extensive and rich ion chemistry occurs even at the ionization threshold energy because the radicals and radical cations generated are very stable, the solvated protons (H₂O)_mH⁺ ($m \geq 3$) and (NH₃)_mH⁺ ($m \geq 1$) are very stable, and the Franck-Condon factor for ionization leaves the cluster ion in a very highly excited vibrational state following the I ← S₁ transition. The latter situation arises because the S₀, S₁ cluster geometry for a polar solvent cluster is much different than that of the cluster ion. The cluster ions are very highly energetic due to the vibrational overlap for ionization and the free energy available from the reaction.

D. Cluster Chemistry of Reactive Intermediates: Benzyl Radical.¹³ The techniques enumerated above are also applicable to the study of radical reactions in clusters, whether they are adiabatic or photogenerated diabatic reactions. Even if the cluster reactions take place on the ground-state surface of the reactive intermediate, spectroscopic product analysis can still lead to an understanding of the reactions that have occurred. Spectra of the benzyl radical isolated in a supersonic expansion have appeared,¹⁶ and cluster spectra with argon, nitrogen, methane, ethane, and propane have been published.¹³ These data lead to an understanding of the D₁ and D₂ excited state of the benzyl radical, the cluster shifts for the D₂ (²B₂), D₁ (¹A₂) ← D₀ (¹B₂) transitions, and to an estimation of the binding energies for these clusters. The cluster shift for these features are all to the red and less than 50 cm⁻¹. The binding energies for these clusters range from ca. 300 to 700 cm⁻¹. Figure 19 gives a comparison of the benzyl radical spectrum with those of a few representative (Ar, CH₄, C₂H₆, C₃H₈) nonreactive clusters.

The spectra of potentially reactive clusters such as benzyl radical/alkenes, acetylene, ammonia, and CO₂ have also been explored. The spectra of benzyl radical(C₂H₄)_{1,2}, benzyl radical(C₃H₆)₁, and benzyl radical(C₂H₂)₁ are presented in Figures 20, 21, and 22. These spectra are distinctly different from those of benzyl radical/alkane clusters. Particularly noteworthy are the large shifts, broad features and large apparent binding energies (>2000 cm⁻¹). The spectra are clearly of a benzyl-like radical because of the transition energies involved: CH₃CH₂[•] absorbs around 250 nm and CH₃[•] absorbs around 200 nm.¹⁷ A number of possibilities exist for both adiabatic and diabatic reactions from the D₂/D₁ surfaces. A ground D₀ state reaction is also possible but in this instance sharp spectra (a cold radical) are to be expected.

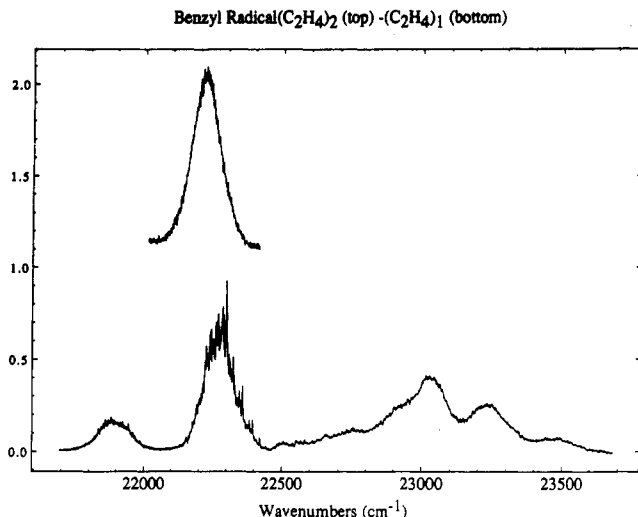


Figure 20. Cluster spectra (two-color MRES) of benzyl radical/ethylene. Note the large binding energy and broad spectrum. The general shapes of the D_2 , $D_1 \leftarrow D_0$ transitions are still visible. Top: $(C_2H_4)_2$. Bottom: $(C_2H_4)_1$.

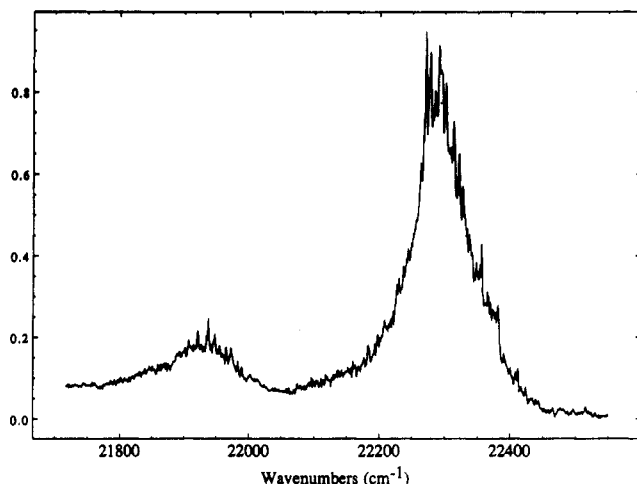


Figure 21. Two-color MRES of benzyl radical (propylene)₁. Note the large binding energy and broad spectrum. The general shape of the D_2 , $D_1 \leftarrow D_0$ transitions are still visible.

Solution-phase studies¹⁸ would suggest that the benzyl radical would react with alkenes and alkynes to form new radicals, which, following [1,2] and [1,3] hydrogen shifts, could then produce substituted benzyl radicals.

We are presently exploring isotopically (H/D) and chemically (F, CH₃, NH₂) substituted precursors to elaborate the behavior of these clusters further. We are also generating various possible product species (e.g., C₆H₅CHR and C₆H₅CH₂R*) in order to identify and characterize the cluster spectra obtained.

Conclusions

For nonreactive systems, structure and dynamics can be studied for isolated and solvated systems using supersonic cooling and mass-, time-, and wavelength-resolved spectroscopy. One can do the same set of studies for elucidation of the structure and dynamics of chemically reacting systems. The effects of energy, isotopic and chemical substitution, solvation, and cluster size and structure can be explored for many different types of reactions. Additionally, the advantage of controlled solvation cluster systems can lead to a real theoretical understanding of reaction mechanisms, pathways, and potential energy surfaces. Good models (potential surfaces) can be found to characterize observations qualitatively and quantitatively. Reactive intermediates (radicals, etc.) can be investigated, as well.

The study of chemical reactions in clusters promises to be an essential component in the elucidation of condensed-phase chemical

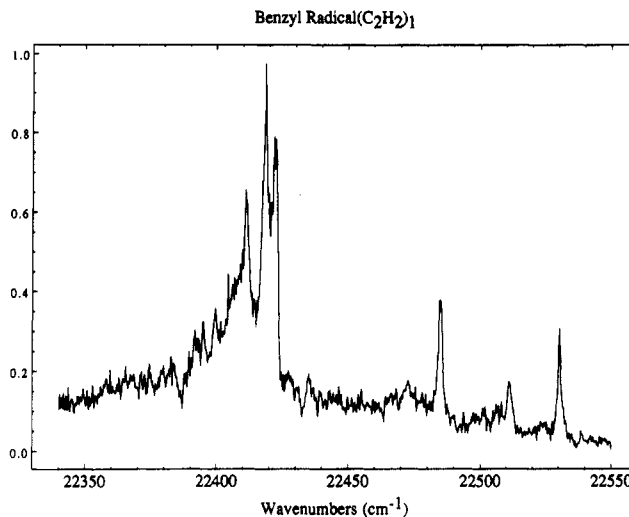


Figure 22. Two-color MRES of benzyl radical (acetylene)₁. This spectrum is very different from the bare radical spectrum. No lower energy features can be found for this cluster system.

reactivity. In particular, results for both electron- and proton-transfer reactions in clusters can address issues dealing with minimum solvation number for reaction, critical solvation geometry, and reactivity as a function of energy. These are all important factors for reactions in condensed phases.

Acknowledgment. Many students, postdoctoral fellows, and colleagues have contributed to the studies discussed in the report and to my understanding of these subjects. In particular I would like to express my debt to Prof. D. F. Kelley and Drs. Q. Y. Shang, S. Li, M. F. Hineman, H. S. Im, and R. Disselkamp. This work is supported by grants from ONR and NSF.

Registry No. DMABN, 1197-19-9; C₆H₅CH₂*, 2154-56-5; 1-naphthol, 90-15-3; toluene, 108-88-3; benzyl alcohol, 100-51-6; α,α -dimethylbenzyl alcohol, 617-94-7.

References and Notes

- (1) (a) Levy, D. H. *Adv. Chem. Phys.* **1981**, *47*, (Part 1), 323. (b) *Atomic and Molecular Clusters*; Bernstein, E. R., Ed.; Plenum: New York, 1990. (c) Bernstein, E. R. *Ibid.* p 551.
- (2) (a) Warren, J. A.; Bernstein, E. R.; Soeman, J. I. *J. Chem. Phys.* **1988**, *88*, 871. (b) Grassian, V. H.; Warren, J. A.; Bernstein, E. R. *J. Chem. Phys.* **1989**, *90*, 3994. (c) Shang, Q.-Y.; Bernstein, E. R. *J. Chem. Phys.*, in press.
- (3) (a) Chesnovsky, O.; Leutwyler, S. *J. Chem. Phys.* **1988**, *88*, 4127. (b) Knochenmuss, R.; Leutwyler, S. *J. Chem. Phys.* **1989**, *91*, 1268. (c) Jouvot, C.; Dedonder-Lardeux, C.; Viaro, M. Richard; Solgadi, D.; Tramer, A. *J. Chem. Phys.* **1990**, *94*, 5041. (d) Syage, J. A.; Steadman, J. *J. Chem. Phys.* **1991**, *95*, 2497. Steadman, J.; Syage, J. A. *J. Am. Chem. Soc.* **1991**, *113*, 6786; *J. Phys. Chem.* **1991**, *95*, 10326. (e) Breen, J. J.; Peng, L. W.; Willberg, D. M.; Heikal, A.; Cong, P.; Zewail, A. H. *J. Chem. Phys.* **1990**, *92*, 805. (f) Loison, J. C.; Dedonder-Lardeux, C.; Jouvot, C.; Solgadi, D. *J. Phys. Chem.* **1991**, *95*, 9192.
- (4) (a) Vaida, V.; Donaldson, D. J.; Sapers, S. P.; Naaman, R.; Child, M. S. *J. Phys. Chem.* **1989**, *93*, 513. (b) Donaldson, D. J.; Vaida, V.; Naaman, R. *J. Phys. Chem.* **1988**, *92*, 1204; *J. Chem. Phys.* **1987**, *87*, 2522. (c) Martrenchard, S.; Jouvot, C.; Dedonder-Lardeux, C.; Solgadi, D. *J. Phys. Chem.* **1991**, *95*, 9186.
- (5) (a) Nimlos, M. R.; Kelley, D. F.; Bernstein, E. R. *J. Phys. Chem.* **1989**, *93*, 643. (b) Kim, S. K.; Li, S.; Bernstein, E. R. *J. Chem. Phys.* **1991**, *95*, 3119. (c) Kim, S. K.; Hsu, S. C.; Li, S.; Bernstein, E. R. *J. Chem. Phys.* **1991**, *95*, 3290. (d) Hineman, M. F.; Bruker, G. A.; Kelley, D. F.; Bernstein, E. R. *J. Chem. Phys.* **1992**, *96*, 3341.
- (6) Turro, N. J. *Modern Molecular Photo Chemistry*; Benjamin/Cummings: Menlo Park, CA, 1978.
- (7) (a) Wittig, C.; Sharpe, S.; Beaudet, R. A. *Acc. Chem. Res.* **1988**, *21*, 341. (b) Bohmer, E.; Shin, S. K.; Chen, Y.; Wittig, C. *J. Chem. Phys.* **1992**, *97*, 2536.
- (8) (a) Scherer, N. F.; Sipes, C.; Bernstein, R. B.; Zewail, A. H. *J. Chem. Phys.* **1990**, *92*, 5239. (b) Scherer, N. F.; Kundkhar, L. R.; Bernstein, R. B.; Zewail, A. H. *J. Chem. Phys.* **1987**, *87*, 1451. (c) Gruebele, M.; Sims, I. R.; Potter, E. D.; Zewail, A. H. *J. Chem. Phys.* **1991**, *95*, 7763.
- (9) (a) Breen, J. J.; Tzeng, W. B.; Kilgore, K.; Keesee, R. G.; Castleman, A. W., Jr. *J. Chem. Phys.* **1990**, *90*, 11, 19. (b) Keesee, R. G.; Castleman, A. W., Jr. *Atomic and Molecular Clusters*; Bernstein, E. R., Ed.; Plenum: New York, 1990; p 507.
- (10) (a) Wei, S.; Tzeng, W. B.; Castleman, A. W., Jr. *J. Phys. Chem.* **1991**, *95*, 5080; **1990**, *92*, 332; *J. Chem. Phys.* **1990**, *93*, 2506. (b) Coolbaugh, M. T.; Vaidyanathan, G.; Peifer, G.; Garvey, W. R., Jr. *J. Phys. Chem.* **1991**,

- 95, 8337. (c) Whitney, S. G.; Coolbaugh, M. T.; Vaidyanathan, G.; Garvey, W. R., Jr. *J. Phys. Chem.* **1991**, *95*, 9625. (d) Alexander, M. L.; Levinger, N. E.; Johnson, M. A.; Ray, D.; Lineberger, W. C. *J. Chem. Phys.* **1988**, *88*, 6200. (e) Ray, D.; Levinger, N. E.; Papanikolas, J. M.; Lineberger, W. C. *J. Chem. Phys.* **1989**, *91*, 6533. (f) Posey, L. A.; Campagnola, P. J.; Johnson, M. A.; Lee, G. H.; Eaton, J. G.; Bowen, K. H. *J. Chem. Phys.* **1989**, *91*, 6536. (g) Papanikolas, J. M.; Gord, J. R.; Levinger, N. E.; Ray, D.; Vorsa, V.; Lineberger, W. C. *J. Phys. Chem.* **1991**, *95*, 8028. (h) Posey, L. A.; Deluca, M. J.; Campagnola, P. J.; Johnson, M. A. *J. Phys. Chem.* **1989**, *93*, 1178.
- (11) (a) Shida, T. *Annu. Rev. Phys. Chem.* **1991**, *42*, 55. (b) Mikami, N.; Sasaki, T.; Sato, S. *Chem. Phys. Lett.* **1991**, *180*, 431. (c) Maeyama, T.; Mikami, N. *J. Phys. Chem.* **1991**, *95*, 7197; *Ibid.* **1990**, *94*, 6973. (d) Rieln, C.; Lahmann, C.; Brutschy, B. *J. Phys. Chem.* **1992**, *96*, 3626. (e) Brutschy, B. *J. Phys. Chem.* **1990**, *94*, 8637.
- (12) Bernstein, E. R.; Law, K.; Schauer, M. *J. Chem. Phys.* **1984**, *80*, 207, 634.
- (13) Disselkamp, R.; Bernstein, E. R. *J. Chem. Phys.*, to be published.
- (14) Li, S.; Bernstein, E. R. *J. Chem. Phys.* **1992**, *97*, 792, 804, 0000.
- (15) Newton, M. D.; Sutin, N. *Annu. Rev. Phys. Chem.* **1984**, *35*, 437. Sutin, N. *Prog. Inorg. Chem.* **1986**, *30*, 441. Closs, G. L.; Miller, J. R. *Science* **1988**, *240*, 440. Marcos, R. A.; Sutin, N. *Biochim. Biophys. Acta* **1985**, *811*, 265.
- (16) (a) Foster, S. C.; Miller, T. A. *J. Phys. Chem.* **1989**, *93*, 5586 and references therein. (b) Lin, T. Y. D.; Damo, C. P.; Dunlop, J. R.; Miller, T. A. *Chem. Phys. Lett.* **1990**, *168*, 349. (c) Fukushima, M.; Obi, K. *J. Chem. Phys.* **1990**, *93*, 8488. (d) Im, H. S.; Bernstein, E. R. *J. Chem. Phys.* **1991**, *95*, 6326.
- (17) Herzberg, G. *Spectra and Structure of Simple Free Radicals*; Cornell University Press: Ithaca, NY, 1971; *Electronic Spectra and Electronic Structure of Polyatomic Molecules*; Van Nostrand: New York, 1966.
- (18) (a) Goumari, A.; Pauwels, J. F.; Sawerysyn, J. P.; Devolder, P. *Chem. Phys. Lett.* **1990**, *171*, 303. Ebata, T.; Obi, K.; Tanaka, I. *Chem. Phys. Lett.* **1981**, *77*, 480. Nelson, H. H.; McDonald, J. R. *J. Phys. Chem.* **1982**, *86*, 1242. (b) Kochi, J. *Free Radicals*; Wiley: New York, 1973.

ARTICLES

Intramolecular Triplet Energy Transfer of the System Having Donor and Acceptor at the Chain Ends. 2. The Carbazole-Naphthalene System

Hideaki Katayama, Shinzaburo Ito, and Masahide Yamamoto*

Department of Polymer Chemistry, Faculty of Engineering, Kyoto University, Sakyo-ku, Kyoto 606, Japan
(Received: April 27, 1992; In Final Form: July 29, 1992)

Intramolecular triplet-triplet (T-T) energy transfer in a series of polymethylene chains having a carbazole group as an energy donor and a naphthalene group as an energy acceptor has been studied by phosphorescence measurement. The phosphorescence decay curves were analyzed by Dexter's equation in which the distribution of donor-acceptor (D-A) distance was calculated by the conformational energy analysis. The results of the simulation were in fairly good agreement with the experimentally observed decay curves. We conclude that the through-space mechanism is adequate for intramolecular T-T energy transfer of the flexible D-A molecules.

Introduction

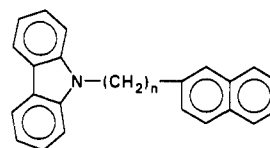
Triplet-triplet (T-T) energy transfer is a basic photophysical process which has been extensively studied since the mechanism was proposed by Dexter.¹ T-T energy transfer is forbidden by the dipole-dipole mechanism but is allowed by the exchange mechanism.² Therefore, the rate constants are highly sensitive to the distance of separation between donor and acceptor.³

Several studies on intramolecular T-T energy transfer have been reported,⁴ but few have measured the rate constants of T-T energy transfer.⁵⁻⁷ Recently, Closs et al. investigated the bichromophoric compounds connected by a rigid spacer and estimated the rate constant of T-T energy transfer in benzene solution at room temperature, by using picosecond laser photolysis.⁶ They concluded that the T-T energy-transfer process occurs via the σ -bond of the spacer (through-bond mechanism).

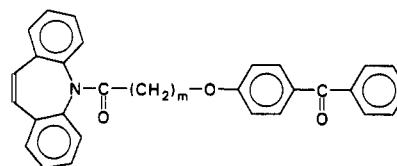
We previously studied the intramolecular T-T energy transfer of the bichromophoric compounds connected by flexible methylene units using a system having a benzophenone (BP) group as an energy donor and dibenz[b,f]azepine (DBA) group as an energy acceptor.⁷ Analysis of the phosphorescence decay curves by Dexter's equation in which the distribution of the donor-acceptor distance was calculated by the conformational energy analysis revealed that the T-T energy-transfer process of flexible D-A molecules obeys Dexter's equation (through-space mechanism).

In the present work, another system of intramolecular T-T energy transfer will be discussed. The sample used here is a series

of polymethylene chains having a carbazole (Cz) group as an energy donor and naphthalene (Np) group as an energy acceptor.



Cz-n-Np



Bp-m-DBA

These compounds are denoted by Cz-*n*-Np (*n* = 8-12), each numeral representing the number of methylene units for each polymethylene chain. This system has the following characteristics: (a) the spacer is composed of simple methylene units, while the previous one has ether and carbonyl groups, (b) the decay profile of the isolated donor (Cz) is single exponential, (c) both the donor and the acceptor reactivities are much less than those of the previous system, and (d) the acceptor (Np) emits phosphorescence,